Resilient Cities and Structures 4 (2025) 1–15

Contents lists available at ScienceDirect

Resilient Cities and Structures

journal homepage: www.elsevier.com/locate/rcns

Full Length Article

Stochastic response of steel columns subjected to lateral blast based on modified single degree of freedom (MSDOF) method

Mohammad Momeni[a,*], Chiara Bedon[b], Mohammad Ali Hadianfard[c], Sina Malekpour[c]

[a] Department of Civil Engineering, Faculty of Engineering, Fasa University, Fasa, Iran
[b] Department of Engineering and Architecture, University of Trieste, Trieste, Italy
[c] Department of Civil and Environmental Engineering, Shiraz University of Technology, Shiraz, Iran

ARTICLE INFO

Keywords:
Stochastic response
Steel column
Lateral blast
Uncertainty
Modified single degree of freedom (MSDOF) method
Parametric analysis

ABSTRACT

This paper aims to evaluate the stochastic response of steel columns subjected to blast loads using the modified single degree of freedom (MSDOF) method, which assessed towards the conventional single degree of freedom (SDOF) and the experimentally validated Finite Element (FE) methods (LSDYNA). For this purpose, special attention is given to calculating the response of H-shaped steel columns under blast. The damage amount is determined based on the support rotation criterion, which is expressed as a function of their maximum lateral mid-span displacement. To account for uncertainties in input parameters and obtain the failure probability, the Monte Carlo simulation (MCS) method is employed, complemented by the Latin Hypercube Sampling (LHS) method to reduce the number of simulations. A parametric analysis is hence performed to examine the effect of several input parameters (including both deterministic and probabilistic parameters) on the probability of column damage as a function of support rotation. First, the MSDOF method confirms its higher accuracy in estimating the probability of column damage due to blast, compared to the conventional SDOF. The collected results also show that uncertainties of several input parameters have significant effects on the column behavior. In particular, geometric parameters (including cross-sectional characteristics, boundary conditions and column length) have major effect on the corresponding column response, in the same way of input blast load parameters and material properties.

1. Introduction

Steel structures are widely favored in construction, being one of the most prevalent materials in building projects. This is especially true in environments where the imperative to conserve space is paramount, making steel a good choice for its versatility and efficiency in design. In recent decades, the perceived risks of various loads (like blast, earthquake, fire, etc.) on different structures have significantly increased [1–10]. Blast loads from explosions create intense, short-duration pressure waves that impact structures, with their effect diminishing as the distance from the explosion increases. This localized nature means that structural members closer to the explosion experience higher pressures and greater potential damage, while those farther away face reduced loads and damage. Analyzing these effects is critical for understanding the overall response of a structure under blast conditions. By studying the behavior of key structural members, such as columns, engineers can assess how the entire structure might react to a blast and determine the likelihood of collapse. Effective blast-resistant design relies on strategic features that help dissipate energy and prevent progressive failure, ensuring the resilience and safety of structures subjected to blast loads. In this regard, the blast performance assessment of structures (mostly structural members) has become a necessary step in design and a critical focus of research [11–19]. Some experiments, documented in the literature [20–23], have been conducted to evaluate the response of steel columns under various blast loads. In terms of numerical studies, researchers have often implemented equivalent single degree of freedom (SDOF) systems or the finite element (FE) method to calculate the response of blast loaded steel columns [22,24–32]. To enhance the accuracy of SDOF method, certain researchers [27,33,34] have incorporated nonlinear resistance functions into the equation of motion for blast loaded steel columns. This modification has led to the proposal of an equivalent modified single degree of freedom system (MSDOF), replacing the conventional SDOF approach. In the MSDOF method, the use of nonlinear resistance function allows the designer to more accurately consider the effects of axial load on the reduction of column flexural capacity for a given steel column. This improvement brings numerical analyses closer to reality. Despite the availability of several deterministic methods for analyzing blast-loaded structures, these methods are not able to account for uncertainties in problem parameters, such as blast loads and material properties. This is due to the fact that deter-

* Corresponding author.
E-mail address: m-momeni@fasau.ac.ir (M. Momeni).

https://doi.org/10.1016/j.rcns.2024.12.001
Received 1 August 2024; Received in revised form 8 November 2024; Accepted 4 December 2024

ministic methods provide a single solution based on fixed input values. In response to this limitation, numerous studies have focused on the reliability analysis of structures under impulsive loads, taking into consideration the uncertainties associated with material properties and blast parameters. These investigations cover a wide range of structures, including steel buildings [35], reinforced concrete (RC) buildings [36–38], RC beams [39], RC columns [40–43], RC wall panels [44,45], RC slabs [46,47], composite walls [48], masonry walls [49,50], clamped aluminum plates [51], profiled wall structures [52] and steel columns [53–55]. Additionally, various studies have explored blast loading variability for incorporation into structural reliability analyses [40,46,56–60]. While many of these studies have utilized the Monte Carlo simulation (MCS) method in conjunction with SDOF, multi degree of freedom (MDOF) and full 3D FE models, none have employed the MSDOF method to determine the probabilistic response of steel columns exposed to blast.

The MSDOF offers several advantages in the analysis of steel columns subjected to explosions. These include reduced computational cost (i.e., faster analysis time) and the ability to handle large-scale simulations for target structures. Overall, these benefits make the MSDOF particularly suitable for conducting probabilistic analyses, with increased accuracy compared to SDOF method. Although it is clear that FE simulations can provide more detailed results, especially when considering localized failure modes (such as shear, bending, or local buckling), they are almost recommended when a more comprehensive understanding of column behaviors is required (i.e., stress distribution, strain pattern, etc.). In this regard, the MSDOF method is advantageous over FE method for probabilistic analyses in which the global response of structures is assessed. It is also essential to recognize that simple methods with one degree of freedom may produce responses that diverge from reality.

Besides, these methods prevail among researchers due to their popularity. A key objective of present investigation is thus to substantiate this condition and promote the use of MSDOF methods. The stochastic response of steel columns subjected to dynamic blast is investigated. To this aim, the damage amount is calculated based on the support rotation criterion as a function of maximum lateral mid-span displacement of column under blast. To obtain the failure probability and take into account the uncertainties of input parameters, the MCS method is utilized with the Latin Hypercube Sampling (LHS) method, to reduce the number of simulations. Finally, a comprehensive parametric analysis is presented to assess the influence of input parameters on the structural behavior of blast loaded steel columns, by varying input variables (including deterministic and probabilistic parameters) and investigating their impact on the column performance (i.e., probability of column damage).

2. Impulsive blast load

Impulsive dynamic loads are characterized by their rapid application to a structure, lasting for a very short duration. Examples of such loads include those generated by free air bursts, ground shocks from surface and underground explosions, impact of vehicle collision etc. Calculating the response of a structure under impulsive loading is inherently complex, primarily due to the rapid and substantial changes in force over time. Impulsive dynamic loads occur less frequently than more conventional loads like dead and live loads. However, despite their infrequency, the destructive potential of impulsive loads is substantial, leading to significant consequences. Their rapid and intense nature sets them apart, making the assessment of a structure's response under such loads a challenging but crucial task.

For present study, the idealized time history of reflected blast pressure is determined by an instantaneous rise to the peak positive reflected pressure (P_r), which occurs right after detonation. P_r reduces exponentially to the negative phase and it is often defined as [61]:

$$\mathrm{P}_r(t) = C_r \times P_{so}(t) \tag{1a}$$

$$P_{so}(t) = \left(P_0 + P_{so}\left(1 - \frac{t-t_a}{t^+}\right) \exp\left(-\alpha \frac{t-t_a}{t^+}\right)\right) \tag{1b}$$

where P_{so} is the peak overpressure monitored for $t = 0$, P_0 is the ambient atmospheric pressure (101.3 kPa), t^+ and t^- are the positive and negative phase durations; t_a is the arrival time; C_r is reflected pressure coefficient and α is a shape parameter. It is worth mentioning that the reason for using P_r(t) as an input load on the structure is that, after an explosion occurs—often taking place at or near ground level—the interaction between the blast wave and the ground surface results in the amplification of the blast incident pressure (i.e. P_{so}(t)), leading to an amplified pressure known as the reflected pressure. There are many literature formulas to calculate P_{so}, t^+ [62] and α [63] as a function of scaled distance Z ($R/W^{1/3}$, where R is the stand-off distance (in m) and W is explosive charge (in kg of TNT)). For C_r, the proposal by Rankine and Hugoniot [61] defining it as $C_r = (14P_0 + 8P_{so})/(7P_0 + P_{so})$, or the graphs provided by UFC-3-340-02 [64] as a function of angle of incidence and peak overpressure can be used. For the present investigation, the effect of shape function was disregarded (i.e., triangular path) and α was set to zero, and the formulae in [40] was used to express P_r and t_d.

3. Modelling assumptions

3.1. SDOF method

The SDOF system is one of the simplest analytical methods for studying the behavior and vibration of structures under the effect of impulsive dynamic loads. While structural systems have commonly more than one degree of freedom, their global behavior can be expressed by SDOF method with good approximation. The real structure is replaced by an equivalent system with lumped mass m, spring stiffness k and damping c as shown in Fig. 1(a). The SDOF system's response is designed to approximate the main structure's behavior at key control points, typically corresponding to plastic hinges. Blast load can be idealized as a triangular shock with maximum load F_m and positive phase duration t_d (Fig. 1(b)). Additionally, damping is generally negligible, given that has minimum effects on the structural response. According to Fig. 1, the dynamic equation of motion for equivalent SDOF system by considering $c = 0$ can be thus expressed as:

$$m\,y + k\,y = F(t) \tag{2}$$

When the member has elastoplastic behavior, ky is replaced with resistance parameter R_s in Eq. (2), which is equal to ky in the elastic region and R_u after yielding (Fig. 1(c)). In Fig. 1(c), the parameters y_e and y_m stand for yielding and ultimate displacement. For a SDOF system with elastic-plastic behavior, the dynamic equation of motion becomes:

$$m\,y + R_s = F(t) \tag{3}$$

To solve Eq. (3), various methods are available such as graphical solution, pressure-impulse diagram, and numerical step-by-step methods as Newmark's-β, Wilson-θ, central difference etc. [65–67]. In the current study, the equation of motion is solved using the Newmark's-β method with a linear acceleration strategy, where the parameters γ and β assume are set to 1/2 and 1/6, respectively. To calculate the blast response of steel columns using the SDOF method, it is necessary to first determine the equivalent parameters for the SDOF system; specifically, the equivalent mass (Me), equivalent stiffness (Ke), and equivalent force (Fe). These parameters are derived based on transformation factors [68]. By determining K_L and K_M, the equivalent force, the equivalent stiffness, the equivalent strength and the equivalent mass can be obtained as $F_e = K_L \times F$, $K_e = K_L \times k$, $R_e = K_L \times R_s$ and $M_e = K_M \times m$, respectively, which should be placed in Eqs. (2) and (3).

Table 1 summarizes the transformation factors for beams or columns with pinned and fixed boundary conditions. The parameters M_{PC} and M_{PS} are the maximum plastic moment capacities of structural member at mid-span and support; L is the column length; w is the intensity of uniform load; E is the elastic modulus; I is the moment of inertia about bending axis.

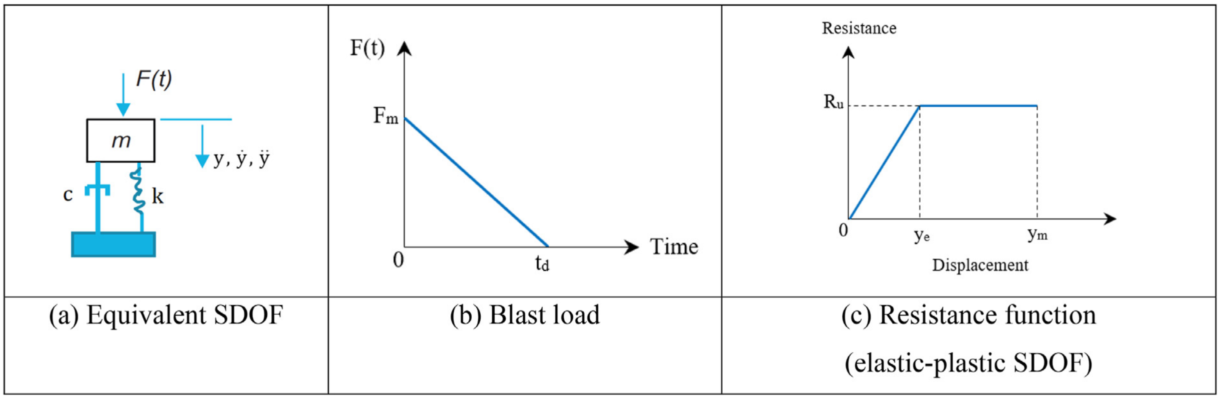

Fig. 1. Example of blast structural analysis based on SDOF method.

Table 1
Transformation factors for beams (or columns) with pinned and fixed boundary conditions under uniform load [68].

Support condition and loading diagram	Strain range	Load factor (K_L)	Uniform mass factor (K_M)	Maximum resistance (R_s)	Spring constant (K)	Dynamic reaction (V)
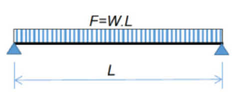	Elastic Plastic	0.64 0.50	0.50 0.33	$8M_{PC}/L$ $8M_{PC}/L$	$384EI/5L^3$ 0	$0.39R_s + 0.11F$ $0.38R_u + 0.12F$
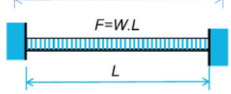	Elastic Elastic-plastic Plastic	0.53 0.64 0.50	0.41 0.50 0.33	$12M_{PS}/L$ $8(M_{PS} + M_{PC})/L$ $8(M_{PS} + M_{PC})/L$	$384EI/L^3$ $384EI/5L^3$ 0	$0.36R_s + 0.14F$ $0.39R_s + 0.11F$ $0.38R_u + 0.12F$

3.2. MSDOF method

The primary distinction between MSDOF and SDOF methods lies in the approach to determining the resistance function of a structural member. In MSDOF, a nonlinear resistance function is employed, deviating from the bi-linear one used in SDOF. This choice not only improves response accuracy but also accounts for the influence of axial force on reducing the strength and stiffness of the member. In essence, the analysis of beam-columns under the effect of a blast differs from the approach taken for beams. Using the energy stability principle, Shope [34] provided an analytical method for designing steel columns under the simultaneous effect of axial and explosive loads. Al-Thairy modified the SDOF method [27,33] by presenting a new nonlinear resistance function of steel columns under transverse blast, based on a quasi-static approximation of column behavior, by taking into account the reduction in the column transverse resistance caused by axial compression. The corresponding nonlinear resistance function is shown in Table 2. It should be noted that for the present study, the blast load is considered as a uniform load applied laterally to the steel column. Given that the nature of explosions involves the expansion and propagation of a blast wave, if the structure is sufficiently distant from the explosion site, the load exhibits a uniform intensity.

In Table 2, U is the maximum transverse displacement and $\eta = 1.4318\ \pi/L$; P is the applied axial load and P_{cr} is the Euler buckling load of the column:

$$P_{cr} = \frac{\pi^2 EI}{\left(K_{eff} L\right)^2} \tag{4}$$

where K_{eff} is the effective length factor (equal to 1.0, 0.5 and 0.7 for columns with pinned ends, fixed ends and fixed-pinned ends).

The elastic-plastic nonlinear flexural resistance function of the column is denoted as $M_{EL\text{-}PL}$. To calculate this function, let's consider a steel column with an H-shaped cross-section exposed to both blast and axial loading, as depicted in Fig. 2. The stress distribution in the cross-section for both negative and positive strains at the bottom layer ($\varepsilon_{\text{t,bottom}}$) is illustrated in Fig. 2(a) and (b). $M_{EL\text{-}PL}$ is obtained by summing up the bending resistance of all the layers over the section depth as:

$$M_{EL-PL} = \sum_{0}^{(h+y_c-y_t)/2} \left(\varepsilon_c E\right) \Delta h\, b_1 \left[\left(h + y_t - y_c\right)/2 + \kappa_1 - \Delta h\right] + \sum_{0}^{(h+y_t-y_c)/2} \left(\varepsilon_t E\right) \Delta h\, b_2 \left[\left(h + y_t - y_c\right)/2 - \kappa_2 + \Delta h\right] - P\frac{h}{2} \tag{5}$$

By considering a linear strain distribution over the cross-section depth, ε_t and ε_c are calculated as follows:

$$\varepsilon_c = \frac{P}{EA} + \phi\, \kappa_1 U \le \varepsilon_y \tag{6}$$

$$\varepsilon_t = \frac{P}{EA} - \phi\, \kappa_2 U \ge -\varepsilon_y \tag{7}$$

The parameter Δh represents the selected layer depth, so that the smaller the value Δh, the higher accuracy of the output. The distance of each layer from the neutral axis in the compressive and tensile regions

Table 2
Elastic and elastic-plastic resistance functions for steel columns with different boundary conditions under the simultaneous effect of axial load and wide blast load along the column.

Boundary	Mode shape equation	Elastic curvature	Elastic resistance	Elastic-plastic resistance
Pin – pin	$u_{(x)} = U \times \sin(\frac{\pi x}{L})$	$\frac{\pi^2}{L^2} U$	$\frac{8.0(P_{cr}-P)U}{L}$	$\frac{8.0(M_{EL-PL}/k-PU)}{L}$
Fix – fix	$u_{(x)} = \frac{U}{2}[1 - \cos(\frac{2\pi x}{L})]$	$\frac{2\pi^2}{L^2} U$	$\frac{8.0(P_{cr}-P)U}{L}$	$\frac{8.0(M_{EL-PL}/k-PU)}{L}$
Pin – fix	$u_{(x)} = \frac{U}{6.2824}[\sin(\eta x) - \eta L \cos(\eta x) + \eta L(1 - \frac{x}{L})]$	$\frac{1.466\pi^2}{L^2} U$	$\frac{8.34(P_{cr}-P)U}{L}$	$\frac{8.34(M_{EL-PL}/k-PU)}{L}$

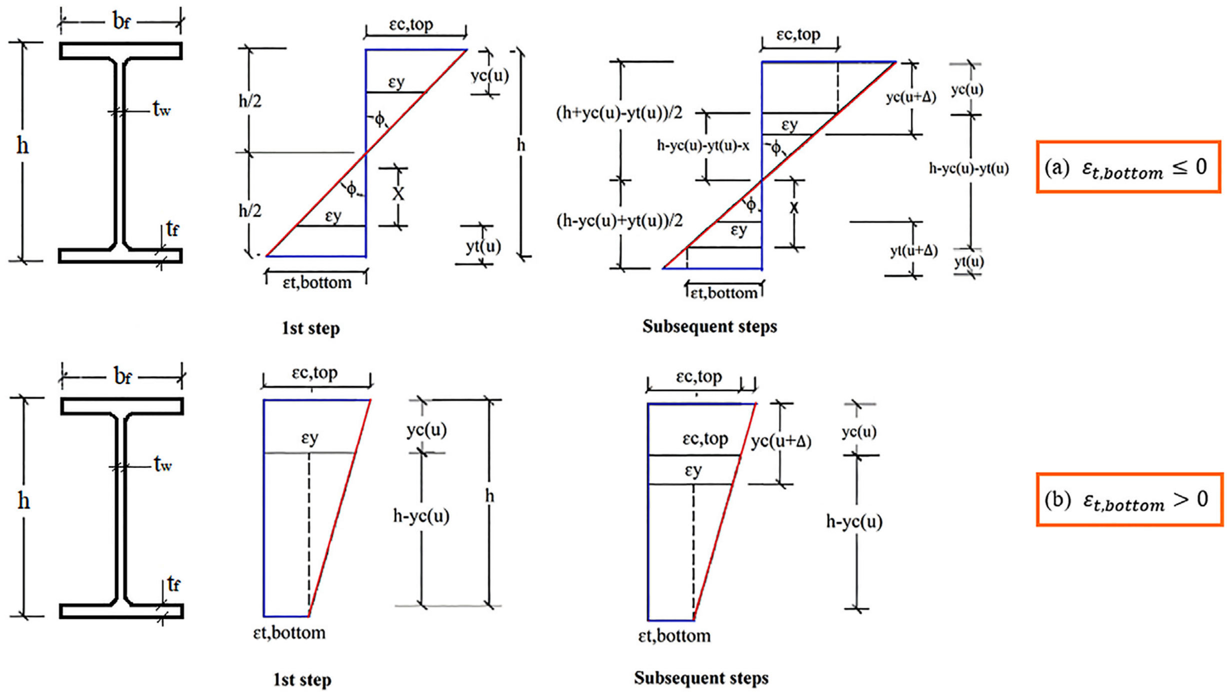

Fig. 2. Strain distribution in the cross section of an H-shaped steel column in bending about major axis [27].

is also determined by the parameters $\kappa_1$and κ_2, respectively. Also, parameters b_1 and b_2 are the width of each layer in the compressive and tensile regions and can be calculated as:

$$\begin{cases} b_1 = t_w \ when \ (h + y_c - y_t)/2 - t_f \geq \kappa_1 \geq 0 \\ b_1 = b_f \ when \ (h + y_c - y_t)/2 \geq \kappa_1 \geq (h + y_c - y_t)/2 - t_f \\ b_2 = t_w \ when \ (h - y_c + y_t)/2 - t_f \geq \kappa_2 \geq 0 \\ b_2 = b_f \ when \ (h - y_c + y_t)/2 \geq \kappa_2 \geq (h - y_c + y_t)/2 - t_f \end{cases} \tag{8}$$

Spread of yielding over the cross section in both tensile and compressive regions is expressed by the parameters y_c and y_t that are given by:

$$y_{c(u+\Delta u)} = y_{c(u)} + \left(h - y_{c(u)} - y_{t(u)} - X_{(u)}\right)\left(1 - \frac{\varepsilon_y}{\varepsilon_{c,Top(u+\Delta u)}}\right) \tag{9}$$

$$y_{t(u+\Delta u)} = y_{t(u)} + X_{(u)}\left(1 - \frac{\varepsilon_y}{\varepsilon_{t,Bottom(u+\Delta u)}}\right) \tag{10}$$

where ε_y is yielding strain of steel, h is section depth and parameters $\varepsilon_{c,Top(u+\Delta u)}$, $\varepsilon_{t,Bottom(u+\Delta u)}$ and $X_{(u)}$ are calculated through Eqs. (11)–(13):

$$\varepsilon_{c,Top(u+\Delta u)avb} = \varepsilon_{axial} + \phi\left(h - y_{c(u)} - y_{t(u)} - X_{(u)}\right) \leq \varepsilon_f \tag{11}$$

$$\varepsilon_{t,Bottom(u+\Delta u)} = \varepsilon_{axial} - \phi X_{(u)} \geq -\varepsilon_f \tag{12}$$

$$X_{(u)} = \frac{h - y_{c(u)} - y_{t(u)}}{\left(1 + \frac{\varepsilon_{c,Top(u)}}{\varepsilon_{t,Bottom(u)}}\right)} \tag{13}$$

where ε_{axial} is the axial strain, ε_f is the fracture strain of steel, $\phi = \partial^2 u(x)/\partial x^2$ is the elastic curvature and $u(x)$ can be defined for different boundary conditions (Table 2). Also, u is the cumulative value of transverse displacement at the previous analysis step, and Δu is the incremental value of the transverse displacement in use for the analysis. When the axial load applied to the column is high and the transverse displacement is small, the position of the neutral axis stands outside the cross-section and the whole column section is subjected to compressive stress as shown in Fig. 2(b). In this case, $y_t = 0$ and y_c is determined as:

$$y_{c(u+\Delta u)} = y_{c(u)} + \left(h - y_{c(u)}\right)\left(1 - \frac{\varepsilon_y - \varepsilon_{c,Bottom(u+\Delta u)}}{\varepsilon_{c,Top(u+\Delta u)} - \varepsilon_{t,Bottom(u+\Delta u)}}\right) \tag{14}$$

The solution of MSDOF equation should be carried out in the following steps of column response:

a) elastic phase:

$$M_e U_{(t)} + R_{EL(U)} = P(t) \ 0 < U(t) < U_{el} \tag{15}$$

b) elastic-plastic phase:

$$M_e U_{(t)} + R_{EL-PL(U)} = P(t) \ U_{el} < U(t) < U_{cr} \tag{16}$$

c) unloading or displacement rebound after elastic phase:

$$M_e U_{(t)} + R_{EL-PL(U=U_R)} - R_{EL(U=U_R-U)} = P(t) \ 0 < U(t) < U_R \tag{17}$$

where U_{el}, U_{cr} and U_R are the displacement at the onset of yielding at the column section, the displacement at which the column fails due to global instability and the displacement at which unloading occurs.

Also, $R_{EL(U=U_R-U)}$ is the elastic transverse resistance function, at the column response $(U_R - U)$ and $R_{EL-PL(U=U_R)}$ is the elastic–plastic transverse resistance function, at the column response U_R.

Fig. 3 shows the nonlinear resistance-displacement function for a steel column. The provided explanations for both SDOF and MSDOF shed light on the differences in analyzing its response under blast.

3.3. Dynamic characteristics of steel material

Structural components undergo significantly higher strain rates when subjected to extreme dynamic loads, such as blasts and impacts, compared to other loads like earthquakes, wind, and live loads. These dynamic loads can rapidly alter the strength characteristics of materials. Typically, the durations of extreme dynamic loads are much shorter than the structural period. To account for the strength increase in materials at high strain rates, the dynamic increase factor (DIF) is applied to

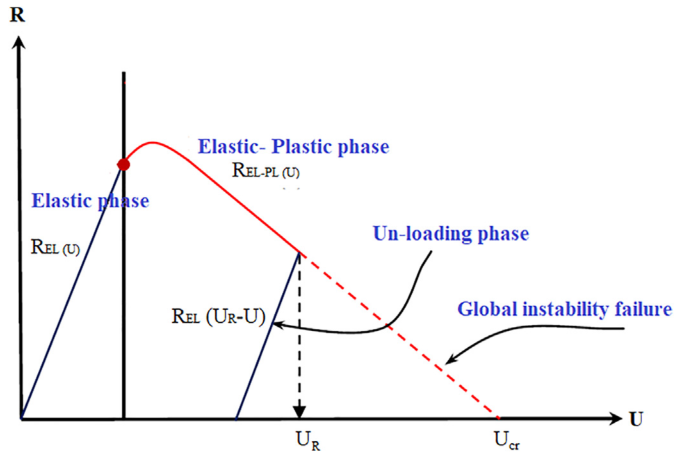

Fig. 3. Generalized nonlinear resistance-displacement function for a steel column [27].

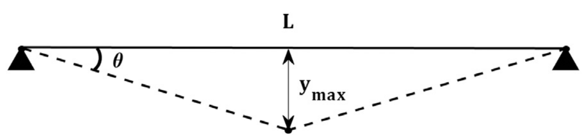

Fig. 4. Schematic model for support rotation criterion.

the static strength values. DIF is defined as the ratio of dynamic strength to static strength of materials and depends on the nature of stress and type of materials [69]. Empirical relationships, graphs, and tables are established in the literature, varying according to the specific type of material. In this study, the strain rate effect of the steel material is accounted for using the Cowper-Symonds relationship, as follows [70]:

$$DIF = \frac{F_{dy}}{F_y} = 1 + \left(\frac{\varepsilon}{C_c}\right)^{\frac{1}{P_c}} \tag{18}$$

where F_y is the static yield stress, F_{dy} is the dynamic yield stress and ε is the strain rate. C_c and P_c are constant values, equal to 40.4 and 5 for mild steel. The dynamic yield stress for steel under extreme dynamic loads is F_{dy} = SIF × DIF × F_y, where SIF = 1.15 for mild steel denotes the strength increase factor [71].

3.4. Damage evaluation based on support rotation criteria

According to performance-based design approach, the amount of deformation in the member to verify determines whether the member has acceptable (or not) response against the imposed extreme load. In this context, the support rotation criterion is one of most common methods in determining the amount of damage caused in a structural member under blast, and relates the maximum deflection y_{max} to the member length L (Fig. 4):

$$\theta = \tan^{-1}\left(\frac{y_{max}}{0.5L}\right) \tag{19}$$

The estimated rotation amplitude in Eq. (19) shall be then compared with a set of limit allowable values θ_{all} given by standards (see Table 3 and [64]), where the support rotation criterion is highly especially for steel members under blast.

In Table 3, two axial load states are also defined, where significant (or not) axial compression load is associated to ±20 % the dynamic axial capacity of the member to verify. To ensure an improved structural performance, stringent values of θ_{all} are recommended for different damage level. Furthermore, the presence of significant axial load, which increases the amount of expected damage originating from P-Δ effects, is associated to more rigid allowable limit values.

Table 3
Maximum allowable support rotation and damage levels for primary steel frame members [64,69].

Significant compressive load	θ_{all} (degrees)		
	Level of damage		
	Low	Medium	High
No	1	2	4
Yes	1	1.5	2

Table 4
Comparison of maximum mid-span displacements.

	Maximum mid-span displacement (mm)						
Test	Experiment	SDOF	Δ (%)	MSDOF	Δ (%)	LS-DYNA	Δ (%)
1	31.36	31.94	+1.8	30.93	−1.4	30.15	−4.0
2	5.34	7.01	+23.8	6.53	+18.2	4.98	−7.2

3.5. Preliminary verification and validation of modelling strategy

In order to validate the MSDOF method, literature experiments have been used, as documented by Nassr et al. [22,72,73]. In addition, MSDOF results are further compared with SDOF (which is written in MATLAB programming as well as MSDOF) and FE analyses based on LS-DYNA software. The experiments involved two samples (named here as Test 1 and Test 2), both utilizing steel column specimens manufactured from W24 × 15 with nominal length of 2.413 m. The specimens were subjected to an axial load of 270 kN and had pinned ends. In Test 1, the explosive charge weight and detonation distance were set to 150 kg of ANFO and 9.0 m. In Test 2, these values were adjusted to 50 kg of ANFO and 10.3 m. Notably, the imposed bending resulting from blast occurred along the strong axis of columns. The setup used in Nassr et al.'s studies [22,72,73] included a concrete frame supporting test specimens and a steel container to house instruments and control blast wave effects. Wing walls minimized blast wave clearance effects. The steel sections, positioned vertically and simply supported, primarily experienced bending stress from blast pressure, with minimal axial stress from self-weight. For further details, see [22,72,73].

For modelling purposes, the material properties, including density, yield stress, elastic modulus, Poisson's ratio, and failure strain, were set to 7850 kg/m^2, 470 MPa, 210 GPa, 0.3, and 0.2, respectively. Input blast parameters, namely pressure and positive phase duration, were determined based on experimental records. The average maximum reflective pressures for Test 1 and Test 2 were found to be 1560 kPa and 307 kPa. Likewise, the average positive phase durations were determined as 6.2 ms for Test 1 and 7.3 ms for Test 2. Consequently, the time-varying load histories in Test 1 and 2 resulted in maximum peak loads of 159.12 N/mm and 31.31 N/mm.

To model the steel column in LS-DYNA software, fully integrated quadrilateral shell elements with five integration points through the thickness of each element were utilized. Shell elements with maximum edge dimensions of 40 mm were chosen. Two rigid plates on the top and bottom of the column were considered to define boundaries and apply the initial axial load as gravity load. Mat_Plastic_Kinematic was adopted for the steel material, which is capable of considering strain rate of material. Additionally, the blast load is applied uniformly throughout the column as a pressure function, utilizing the Segment_Set feature in the software. Given that the primary focus of the present study is on the MSDOF method, a concise explanation of the FE model is provided for brevity. However, for a more comprehensive understanding, additional details can be found in [74,75].

The results of simulations performed by SDOF, MSDOF and LS-DYNA methods for Test 1 and 2 in terms of the maximum lateral mid-span displacements are listed in Table 4.

As Table 4 reveals, in Test 1 $y_{\max}$ for columns modeled by SDOF, MSDOF and FE based LS-DYNA are 31.94, 30.93 and 30.15 mm, which show a negligible scatter of +1.8 %, −1.4 % and −4.0 % with respect to the 31.36 mm displacement of the experiment. In Test 2, an acceptable level of accuracy was observed for FE modelling in predicting the behavior of the steel column with scatter of −7.2 % comparing to experiment. Furthermore, it can be seen that both SDOF and MSDOF methods, with scatter of +23.82 % and +18.2 % to experiments, have good accuracy and efficiency in determining the column response. Although the SDOF and MSDOF methods show some discrepancies compared to experimental and FE results, the idea behind using SDOF methods is to simplify a structure with many degrees of freedom to just one degree of freedom. It's reasonable to assume that this simplification could introduce errors when compared to modeling the structure with FE methods, which use thousands of elements and degrees of freedom. However, many studies in the literature continue to use the SDOF method without accounting for its limitations relative to FE models. While the MSDOF method shows some variability compared to the FE approach, it offers improved accuracy over the conventional SDOF method, thanks to its nonlinear resistance function. Overall, the MSDOF method has higher accuracy than SDOF method and it is implemented in the following stochastic analysis of steel columns under blast loading.

4. Stochastic analysis

4.1. MCS analysis based on LHS method

In order to assess the uncertainties of input random variables in response of steel columns under blast loads, the developed validated deterministic MATLAB code for MSDOF method is further extended for generating probability density functions of input variables and making an iterative calculation based on MCS and LHS methods. The technique of MCS is simple and relatively most accurate widely used method for estimating statistical properties of structural systems under the effect of uncertainties associated with input parameters [76,77].

In the MCS method, the whole system is simulated several times so that all simulations have the same chance of occurring, and each simulation will be a manifestation of the probable behavior of the system. In each simulation and for each input variable, a random value is selected according to the properties of the distribution function for which the variable is intended, and by placing it in the objective function, the value of the objective function is calculated. This process is repeated until enough output values are generated to construct the probability distribution curve of the objective function. It should be noted that finding the probability of damage caused to a steel column under blast load which is the objective function used in this study, where the damage is calculated based on the support rotation criterion. The number of iterations required in the MCS method depends on the level of safety, the desired accuracy for solving the problem, the form of limit state function, and the number of random variables involved in the problem. There are various problems in civil engineering where no closed-form formulation can be found for the limit state function to express the problem. Hence, in many cases the problem being analyzed is more complex, and the time needed to analysis the problem even for a single simulation may be very long, and the time needed to complete many simulations (for reliability analysis) may be unachievable. In this regard, the LHS method is one of the best techniques for reducing the number of simulations needed to obtain reasonable results with the least possible number of simulations. In this method, the range of possible values of each random input variable is divided into a number of "stratum", and a value is randomly selected for each variable from the considered strata as a "representative" value, so that the selected value is considered once and only once in the simulation process. This strategy ensures all possible values of the random variables are presented in the simulation.

In the present study, the MCS and LHS method are used to perform stochastic analysis. The probability of failure based on MCS equals to $P_f = N_f/N$, where N is the number of total simulations and N_f is the number of trials for which limit state function, $g(X) = R{-}Q$, falls in the failure region or has negative value. In doing so, X is the vector of input random variables, R is the capacity or resistance, Q is the demand or loading. The probability of failure can also be written as:

$$P_f = P\left[g(x) \le 0\right] = \int_{G(x)\le 0} f_x(x)dx \, \frac{\sum_{i=1}^{N} I_F\left(x_i\right)}{N} \quad (20)$$

where $f_x(X)$ is the joint probability density function and I_F is the failure indicator which equals 1 if $g(X) \le 0$ and 0 if $g(X) > 0$.

4.2. Uncertainty of input parameters

One of the important issues related to the stochastic analysis of structures is determining the uncertainty associated with input parameters. For steel material, yield stress F_y and elastic modulus E_s are usually considered as random parameters [35,78–81], while the effect of elastic modulus on the failure probability is proved to be almost negligible [54]. Therefore, in present study, E_s is considered as deterministic parameter and F_y is considered as random variable with mean value 240 MPa and coefficient of variation (COV) 0.06. Also, the normal probability density distribution function is used to represent the statistical distribution of F_y.

Geometric uncertainties include the dimensions and size of the steel section, as well as boundaries. The effect of this type of uncertainty can be investigated by considering different states. For example, the support conditions considered for a column in an analysis are idealized (pinned or fixed ends), and in fact in reality the column support conditions are neither fully pinned nor fixed. To consider the uncertainties related to the support conditions, the reliability of columns with fully pinned and fixed ends can be examined and then, based on engineering judgment, an intermediate value can be considered for the actual support condition. There is another approach in which the semi-fixed column support condition can be modeled by translational and torsional springs, and its behavior can be investigated by assigning various translational and torsional stiffnesses. The same procedure can also be followed for columns with different geometries. As an example for considering column length, the reliability analysis can be performed for a number of columns with specific length, and then the probabilistic response of columns with different lengths can be extracted by interpolation [82].

For gravity, the uncertainties are related to the dead and live loads. A random uniform load is used, with a specified mean and standard deviation. In the reliability analysis of columns under extreme loads, axial load is usually equal to 20 % of the initial capacity. Consequently, the initial axial load with mean 20 % of the initial capacity of the member and COV = 0.1 is used in present study, and the normal density function is implemented to express its statistical distribution [35,37,83].

Considering the variability and uncertainties of blast loading parameters is crucial and very important due to the nature of explosion. Several methods can be found in the literature to calculate the uncertainties associated with blast load parameters. Previous works [46,56,84] have documented constant COV values for blast load variability across different scaled distances. Conversely, empirical data and blast test results confirm the inherent variability, prompting additional investigations in [46,56,84]. Notably, the methods proposed by Hao et al. [40] and Netherton and Stewart [57] have broad applicability and find frequent usage in reliability analyses of structures subjected to blast loads. This is because, despite some differences in the cited strategies, they all share a common feature as blast load variability expressed in terms of Z. In addition, the proposed strategies are validated across a broad range of scaled distance values (i.e. 0.24 m/kg$^{1/3}$ $\le Z \le$ 40 m/kg$^{1/3}$ in [40] and 0.59 m/kg$^{1/3}$ $\le Z \le$ 40 m/kg$^{1/3}$ in [57]). In this paper, P_r and t_d are selected as random variables for blast loading, and their variabilities

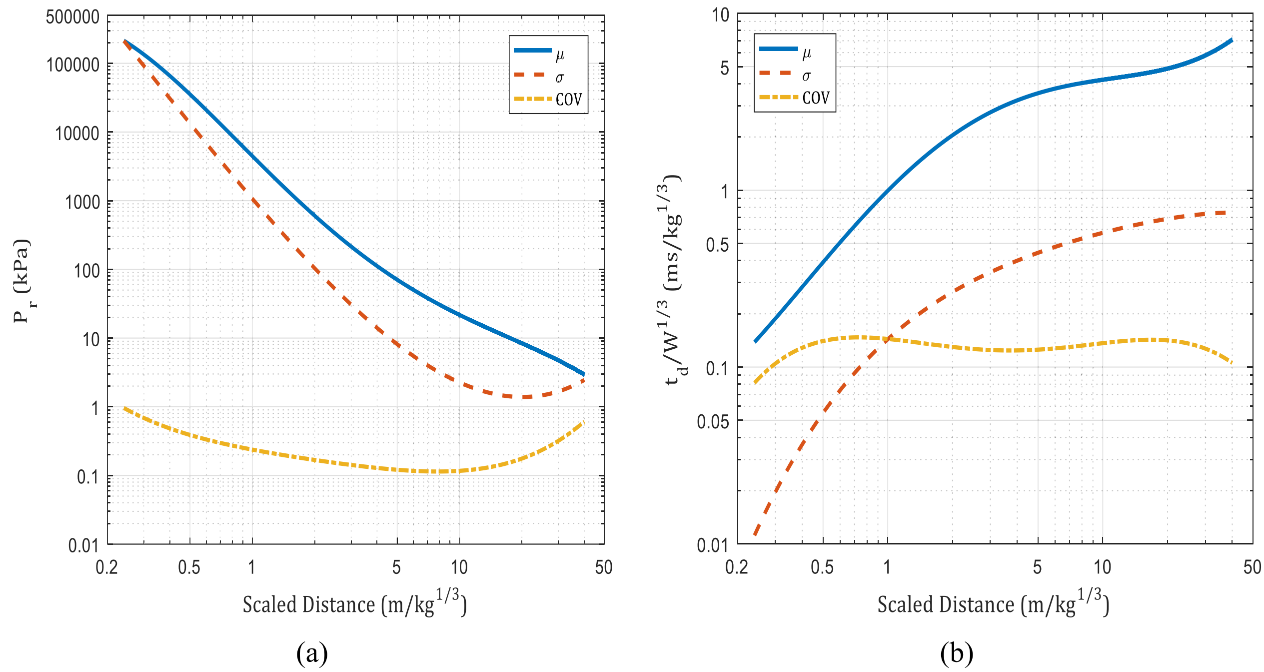

Fig. 5. Mean, standard deviation and COV of (a) peak reflected pressures and (b) normalized positive time duration.

Table 5
Values for coefficients (a_i) in Eq. (21) [40].

Y	a_0	a_1	a_2	a_3	a_4
μ_{P_r}	+3.651	−3.018	+0.1967	+0.8873	−0.3795
σ_{P_r}	+3.03	−3.533	+0.4534	+0.3248	+0.07896
COV_{P_r}	−0.6239	−0.5726	+0.3203	−0.3538	+0.2973
μ_{t_d}	−0.00307	+1.2186	−0.5207	−0.2835	+0.2132
σ_{t_d}	−0.8433	+1.0982	−0.8127	+0.4214	−0.1046
COV_{t_d}	−0.8411	−0.1186	−0.2868	+0.6955	−0.3141

are calculated based on Hao et al. [40]. In this regard, for a blast scenario (with specified charge weight and stand-off distance) the mean, standard deviation (σ) and COV of wave parameters can be estimated as a function of Z as follows:

$$Y = W^{\frac{j}{3}}\ 10^{\left(\sum_{i=0}^{4} a_i \times (\log(Z))^i\right)} \tag{21}$$

where the parameter Y can take mean, standard deviation and COV of reflected pressure and positive time duration, and the coefficients (a_i) can be determined by Table 5. It is worth mentioning that the parameter j in Eq. (21) should be set to 0 and 1 for the calculation of statistical parameters of reflected pressure and positive time duration. Fig. 5(a) and (b) show the statistical characteristics of peak reflected pressure and normalized positive time duration. As reported in [40], Eq. (21) is valid only for an open field explosion and flat reflection surface. For a complex explosion scenario, more significant variations are expected because of blast wave interaction with surrounding structures.

It is also important to note that in some research studies the waveform coefficient has been considered as probabilistic [49,84], but the intended scaled distance was set between 1.62 and 2.78 m/kg$^{1/3}$, and most importantly an explicit relation was not presented for calculation of statistical properties of the waveform coefficient (i.e., mean and standard deviation), based on scaled distance. Following [37,40–42,57,85–91], a linear function is thus used in the present study to define blast history.

5. Numerical analysis and discussion of results

5.1. Calculation example

A steel column with an H-section, featuring a web thickness of 15 mm, flange thickness of 25 mm, flange width of 206 mm, web height of 220 mm, and a length of 3.6 m, is under consideration. The column belongs to a 3-story steel building located in intermediate level of relative seismic hazard in Iran and designed according to [92]. Two different explosion scenarios as Scenario 1 with explosive charge weight of 275 kg of TNT at detonation distance of 13 and Scenario 2 with explosive charge weight of 275 kg of TNT at detonation distance of 14 m are taken into account. The boundary condition for the examined column is assumed to be pinned ends. To conduct the probabilistic analysis, MCS is used with LHS method with 300 simulations in each case. The results of the stochastic analysis, represented as probability functions of support rotation (derived from data histograms), are depicted in Figs. 6 and 7. These results pertain to both blast scenarios and are obtained using MSDOF, SDOF, and LS-DYNA methods.

Figs. 6 and 7 clearly demonstrate that the damage criterion based on support rotation is a non-deterministic parameter, as it is susceptible to uncertainties arising from blast load and material characteristics. The presence of these uncertainties exerts a substantial influence on the resulting support rotation values. It is thus imperative to acknowledge and incorporate these uncertainties when analyzing and interpreting the support rotation data, as they play a crucial role in accurately understanding the behavior and response of a given structural system (damage evaluation) under blast scenarios.

It is important to note that, in each method, a probability density function has been fitted to the obtained histograms to ascertain the probabilistic characteristics of the outputs. In the SDOF method, a normal distribution was fitted to the data, while for the MSDOF and LS-DYNA methods, a log-normal distribution was employed. This choice was influenced by the presence of skewness in the data from the latter two methods, whereas the output from the SDOF method showed a closer resemblance to a normal distribution. As a result, the MSDOF method not only demonstrates superior accuracy in estimating probabilistic parameters, including mean and variance (refer to Fig. 8), but

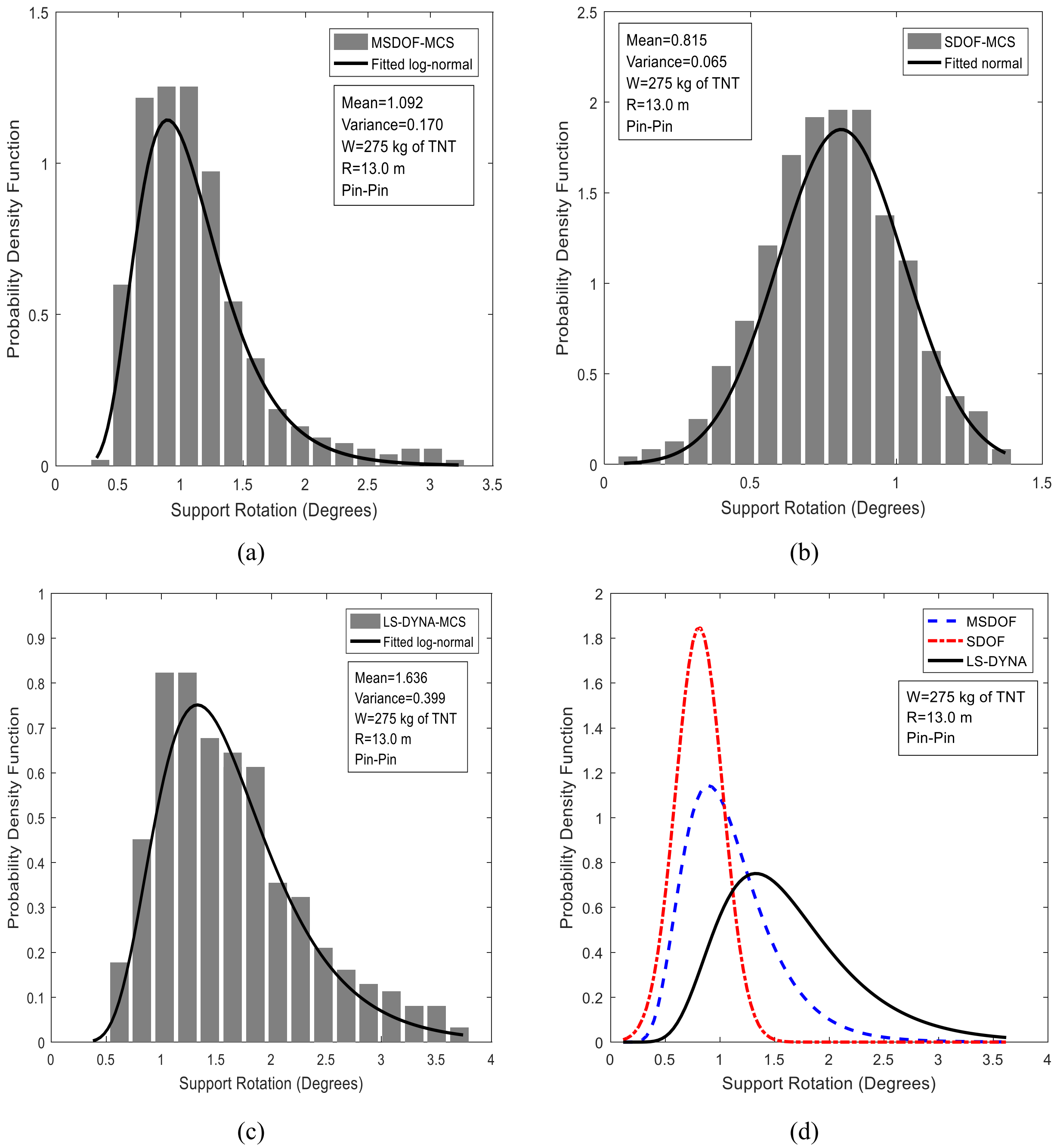

Fig. 6. Support rotation output from MCS for Scenario 1: (a) MSDOF, (b) SDOF, (c) LS-DYNA and (d) comparison between different methods.

also incorporates the nonlinear behavior of the system under blast conditions through the consideration of a nonlinear resistance function. It's noteworthy that although all input variables in the probabilistic analysis adhere to a normal distribution, the resulting outputs deviate from normality. This deviation is attributed to the nonlinearity of the limit state function, particularly evident in MSDOF and LS-DYNA results, which represent the response of the steel column under blast load.

Fig. 9 shows the cumulative distribution functions of the support rotation using SDOF, MSDOF and LS-DYNA methods, which are obtained based on the probability density functions of each case given in Figs. 6 and 7. If the results obtained from FE are assumed to be closer to the reality, based on Fig. 9, it is clear that the MSDOF has higher accuracy in estimating the support rotation probability values than SDOF.

Referring to Fig. 9 and the maximum allowable support rotation values (Table 3), for instance, the probability of low damage (support rotation less than 1 degree) in Scenario 1 is 0.85 for SDOF and 0.62 for MSDOF, showing a difference of 0.66 and 0.43, respectively, compared to the FE method (0.19). In Scenario 2, the probability of low damage is 0.99 for SDOF and 0.93 for MSDOF, with differences of 0.40 and 0.34 compared to FE (0.59). Despite the popularity of the SDOF method due to its limited computational requirements, as seen in the comparative results, the MSDOF method demonstrates improved accuracy in estimating the probability of column failure compared to SDOF. Thus, caution should be exercised when using the SDOF method in probabilistic structural analysis. While MSDOF is more accurate than SDOF, it is important to note that probabilities obtained from both methods still differ from those obtained by the FE method, which demands substantial computa-

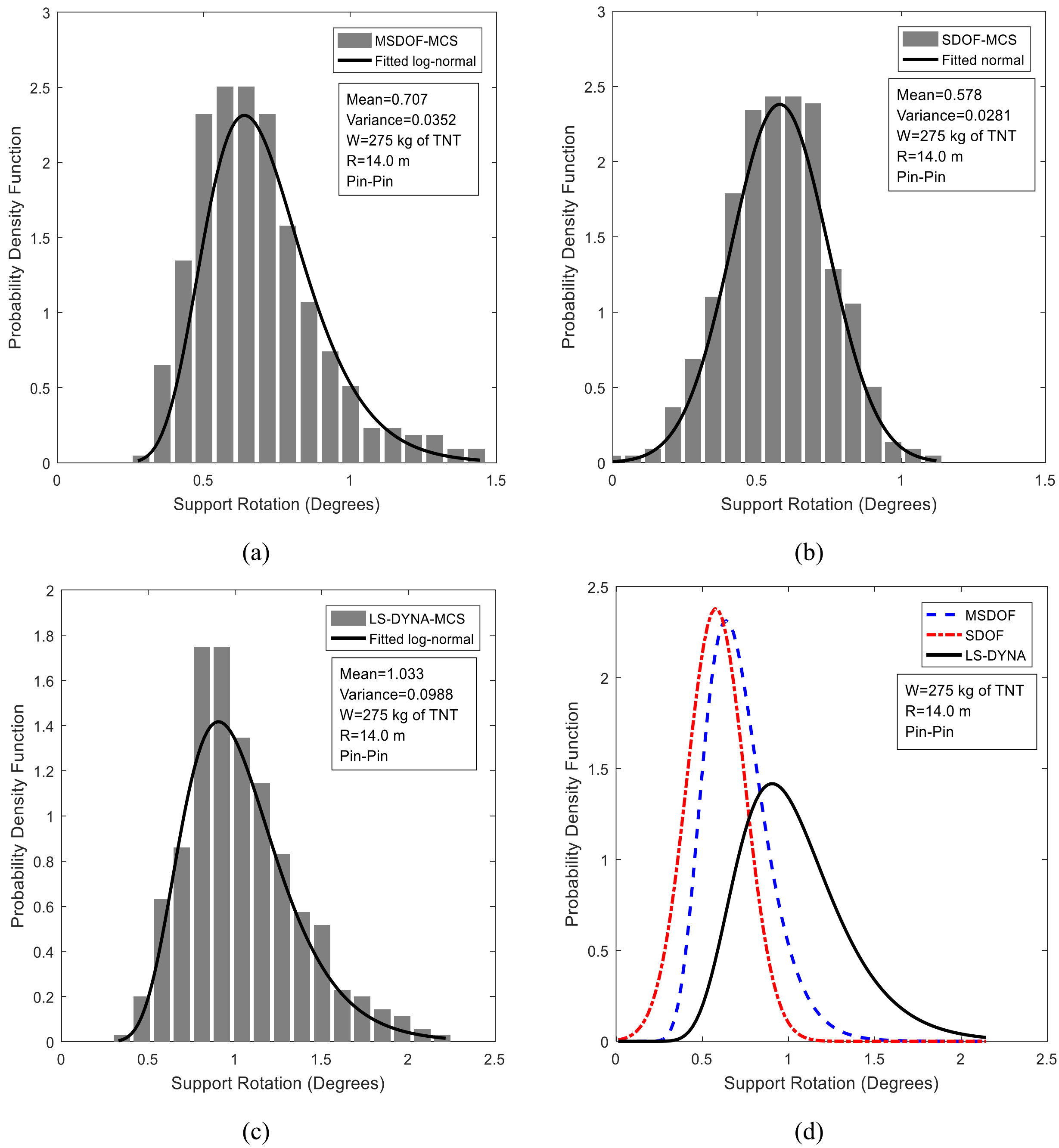

Fig. 7. Support rotation output from MCS for Scenario 2: (a) MSDOF, (b) SDOF, (c) LS-DYNA and (d) comparison between different methods.

tional efforts. The latter approach should be preferred when very high accuracy is essential.

Fig. 10 illustrates the random nonlinear resistance functions of the steel column in Scenario 1, based on 300 simulations. To enhance clarity and observe the effects of uncertainties on the nonlinear resistance function more closely, a zoomed-in view of the rectangular window from Fig. 10(a) is provided in Fig. 10(b). As can be seen from Fig. 10(a) to (b), the uncertainties of input parameters have a significant effect on the resistant function of the steel column, and this leads to a change in the blast response. Such a result can be also clearly deduced from Fig. 11, where the mid-span displacement of the column in Scenario 1 (with 300 simulations) is shown. From Figs. 10, 11, it can be concluded that incorporating uncertainties into the calculation of the response of columns exposed to blast loading is critically important. Such consideration enables a more accurate assessment of structural resilience and safety, emphasizing the potential variations in response under varying conditions.

5.2. Parametric analysis

A parametric sensitivity analysis is also performed to evaluate the response of blast loaded steel column to change of input parameters [93,94], and in particular the influence of fluctuations in input geometric parameters on the outcomes of simulations. In this regard, basic column features such as the cross-sectional characteristics (flange thickness (t_f), flange width (b_f), web thickness (t_w) and web height (h_w)), the material properties (F_y) and also the blast parameters (stand-off distance (R) and charge weight (W)) are considered. The effect of additional pa-

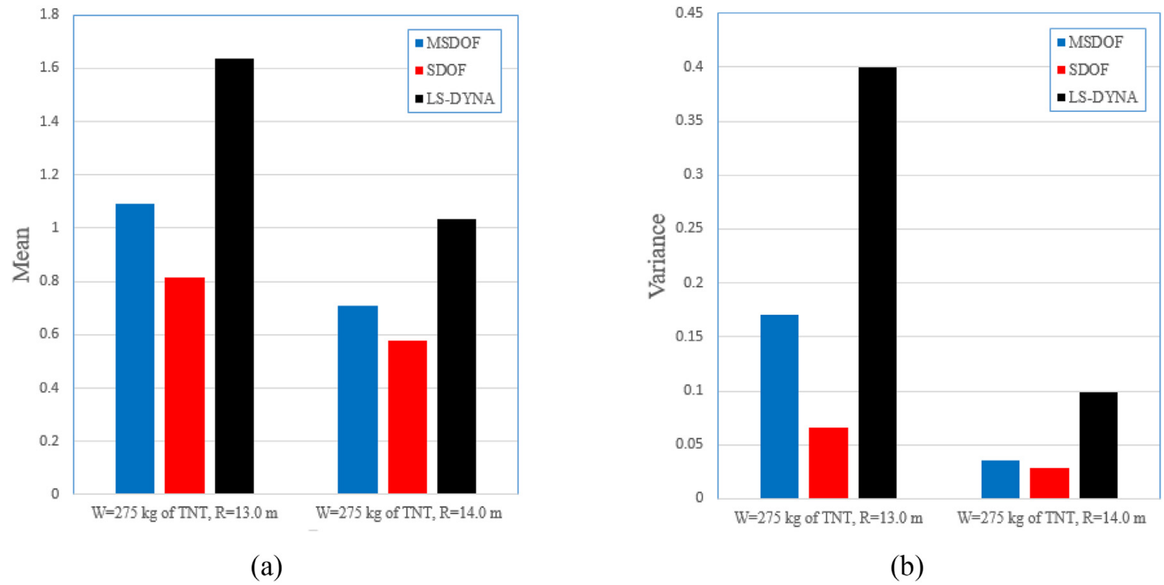

Fig. 8. (a) Mean and (b) variance values obtained by MSDOF, SDOF and LS-DYNA for scenarios 1 and 2.

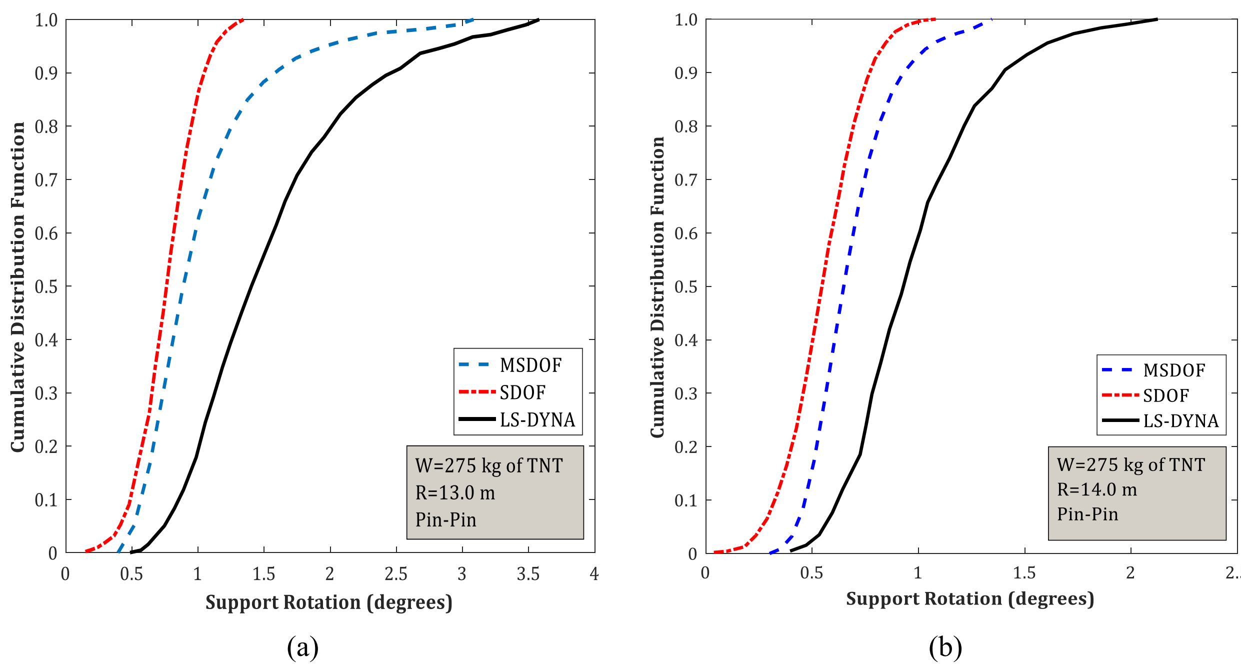

Fig. 9. Cumulative distribution function of support rotation for (a) Scenario1 and (b) 2.

rameters (which were fixed during stochastic analysis) is also considered (i.e. column length (L) and axial load ratio (AL)).

To perform the parametric analysis, input for the above parameters (both certain and uncertain) is changed from 0.85 to 1.15 of their mean value. This range allows to examine a 15 % increase or decrease effect, around the mean value, on the output. By defining this range, it becomes thus possible to observe the ascending, descending, or neutral trends of each input parameter on the output, and gain insights into the effects of this uniform adjustment on the output. It is important to highlight that possible alternative values (like 0.7 to 1.3 etc.) can be taken into account, without impacting the ultimate trend outcome (ascending, descending or neutral trend).

The results of parametric analysis in terms of cumulative distribution function of support rotation are shown in Fig. 12. To evaluate the influence of parameter variation, the value selected for each parameter is changed while the selected values for the other stochastic input parameters are kept unchanged. The amounts of changes in the probability of low damage (support rotation less than 1 degree) corresponding to change in the input parameters are given in Fig. 13.

As shown in Figs. 12 and 13, in case blast load parameters, by increasing in the stand-off distance and charge weight, the probability of low damage respectively increases and decreases. By increasing the axial load, the probability of low damage decreases, which indicates a higher level of damage. For material properties, increasing the yield stress, the probability of low damage increases, and denotes further sensitivity of column. In case of sectional properties, by increasing the flange thickness and width, the probability of low damage decreases and increases

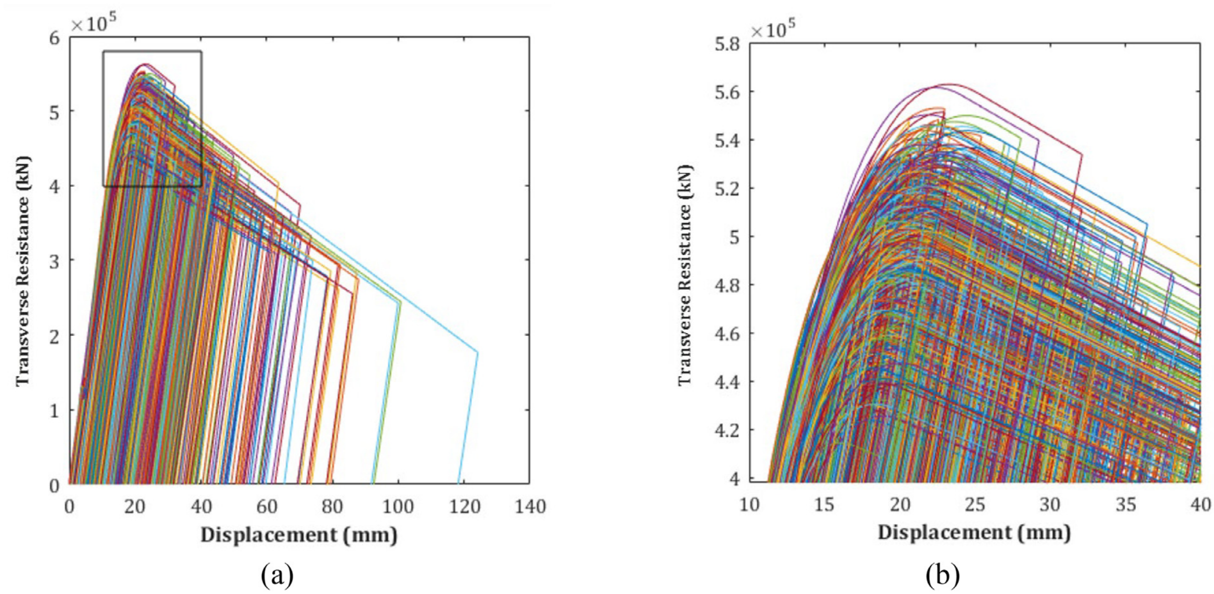

Fig. 10. Stochastic representation of nonlinear resistance function in (a) Scenario 1, with (b) box detail.

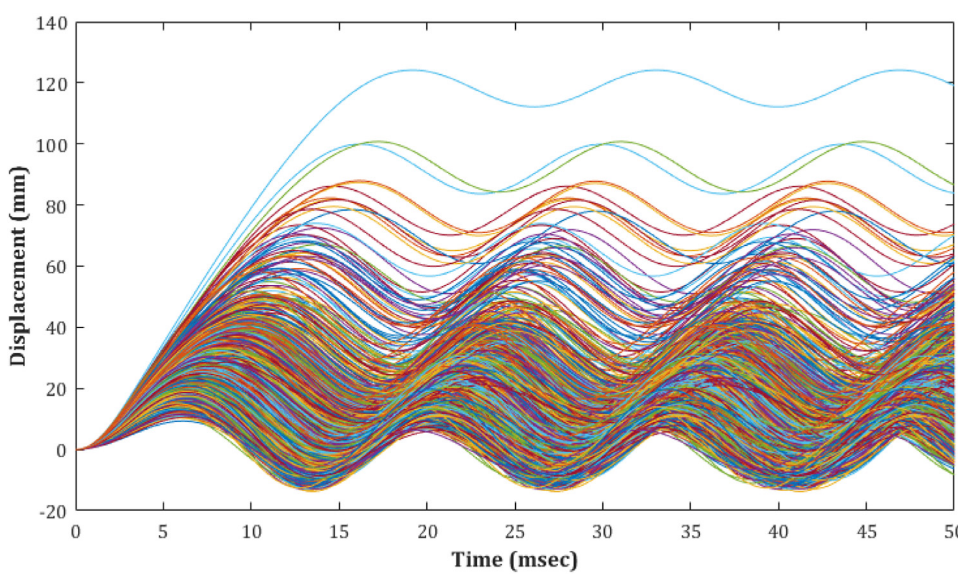

Fig. 11. Stochastic representation of mid-span displacement of selected steel column in Scenario 1.

respectively. This is because as the flange width increases, the load-bearing surface of the column increases, which causes an increased applied force and hence more damage. Similarly, by increasing the web thickness and height, the probability of low damage increases in both cases, but the sensitivity of the model to changes in the web height is a much higher. This is due to the fact that by increasing the web height, the moment of inertia around the bending axis also increases, which ultimately reduces the lateral mid-span displacement and consequently the column damage. As a final case, increasing the column length leads to decrease in the probability of low damage, and thus more severe damage is expected.

As shown in Fig. 13, the parameters including column length, web height, charge weight and stand-off distance are the most sensitive parameters. Although the cross-sectional size parameters are considered as deterministic during the stochastic process, a change in any of these parameters has significant effect on the column response and damage. Therefore, considering the geometry uncertainties of the problem is as important as the uncertainties of input loads and material properties, but few researchers have mentioned this aspect in literature studies.

For existing structures, geometric uncertainties become even more important, and thus higher sensitivity is expected. For example, one of the parameters that can put steel structures at risk is corrosion, especially in coastal areas with high humidity and age-related structural degradation. Corrosion changes the strength of steel, but also causes stress concentration and a change in the thickness of steel components. The effect of corrosion could be thus considered in the response assessment of steel structures by selecting the appropriate distribution functions for the reduced parameters (for example, a log-normal density function for thickness), which may result in accelerating the occurrence of plastic hinges and thus in decreasing the ultimate lateral blast resistance, with lower stiffness and energy dissipation capacity of the specimens. As a nutshell, in the present research, it was shown the importance of geometrical parameters on the damage analysis of steel columns, but the general consideration on uncertainties of these parameters necessarily requires more research.

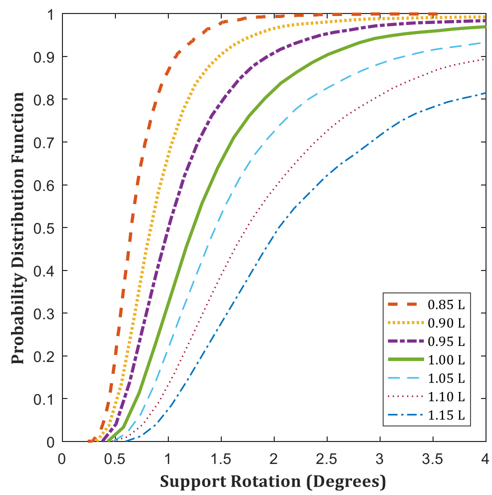

(a)

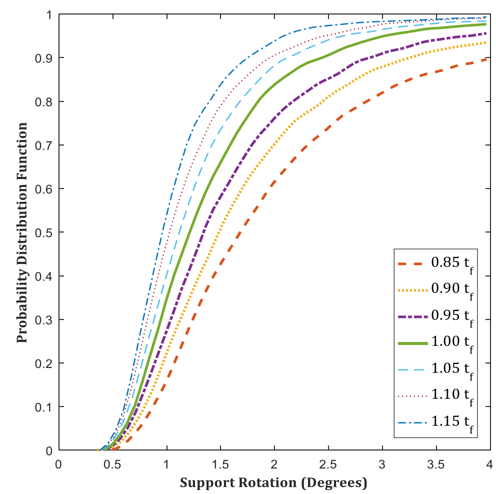

(b)

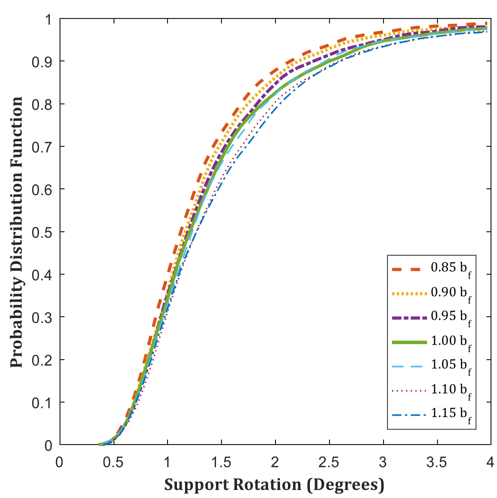

(c)

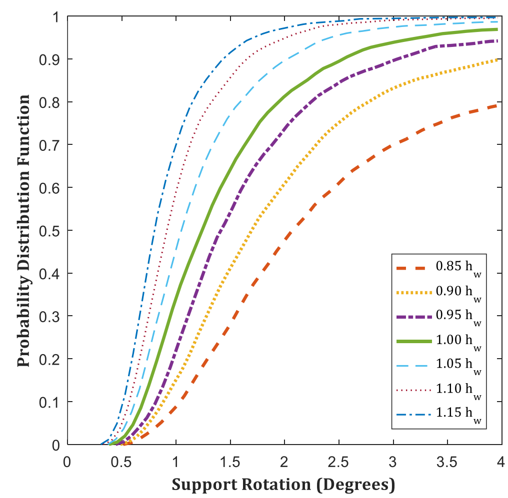

(d)

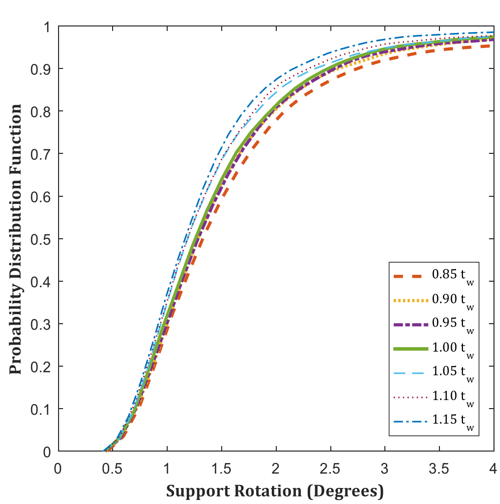

(e)

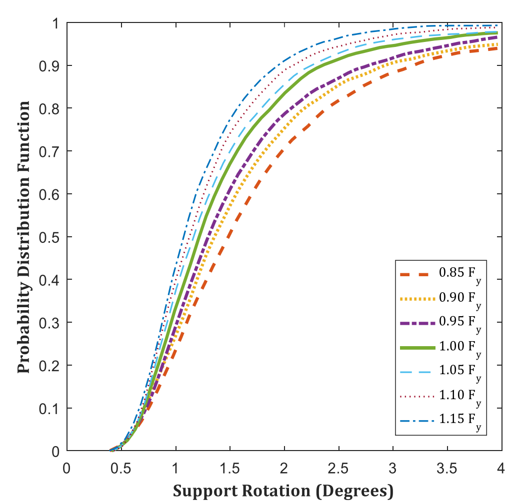

(f)

Fig. 12. Change in probability distribution of support rotation corresponding to change in input parameters in the range of 0.85 to 1.15 of their mean values: (a) L; (b) t_f; (c) b_f; (d) h_w; (e) t_w; (f) F_y; (g) W; (h) R; and (i) AL.

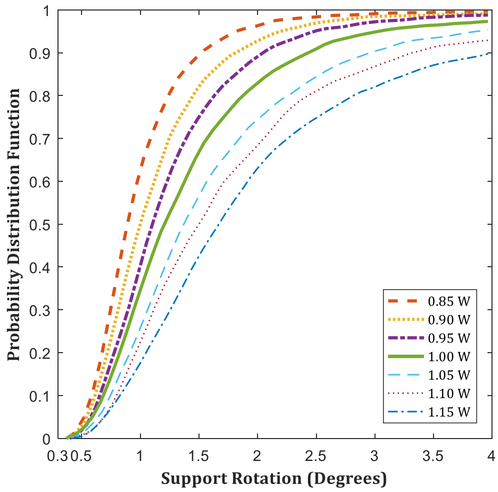

(g)

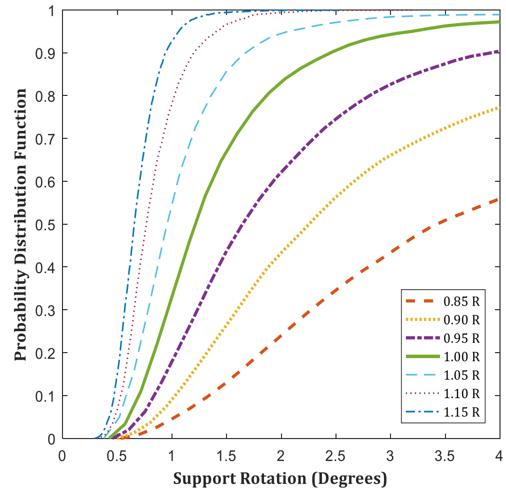

(h)

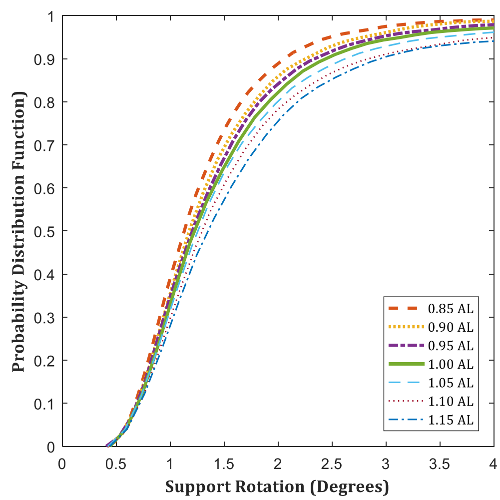

(i)

Fig. 12. Continued

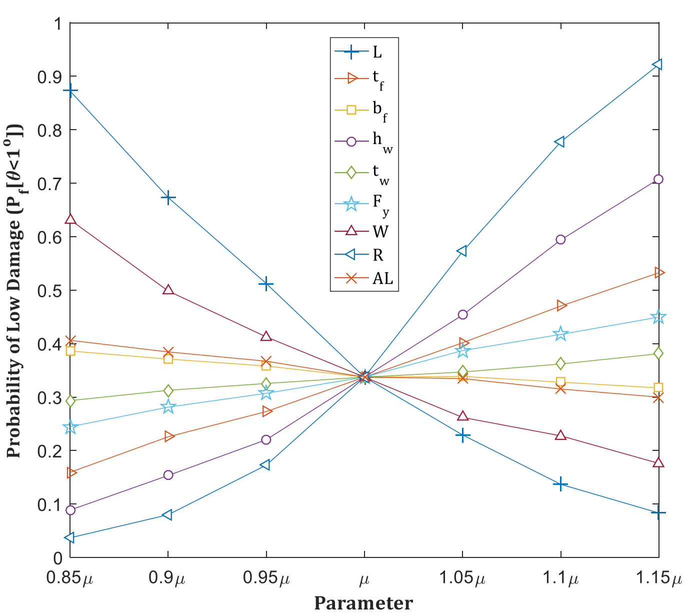

Fig. 13. Results of parametric analyses for all input parameters and their effects on probability of low damage.

6. Conclusions

This study evaluated the stochastic response of steel columns under dynamic blast loads using the modified single-degree-of-freedom (MSDOF) system method, which incorporates a nonlinear resistance function. The MSDOF method was implemented in MATLAB and validated against results from existing experiments. Damage assessment was based on the support rotation criterion, using maximum mid-span displacement as the damage index. To account for uncertainties in input parameters, a stochastic analysis was performed using Monte Carlo Simulation (MCS) with Latin Hypercube Sampling (LHS). In addition to verifying the MSDOF method with experimental data, we compared it with the conventional SDOF and the finite element (FE) method via LS-DYNA software. The results showed that while the MSDOF method has some variability relative to experimental and FE method data, it demonstrates improved accuracy over the conventional SDOF, mainly due to its nonlinear resistance function. Parametric analysis further revealed that uncertainties in input parameters—such as geometric factors, boundary conditions, and material properties—significantly influence column response and damage probability. Specifically, variations in cross-sectional characteristics, boundary conditions, and column length were found to have a comparable effect to blast load parameters and material properties. Additionally, probability functions for support rotation, derived from histogram data, underscored the non-deterministic nature of the damage criterion, highlighting its sensitivity to uncertainties in blast loads and material characteristics. Although all input variables were modeled with normal distributions, output deviations from normality indicated the influence of the nonlinear limit state function, particularly in simulations using the MSDOF and FE approaches.

Relevance to resilience

The findings from this study highlight key aspects of structural resilience by demonstrating how steel columns respond to blast loads under uncertain conditions. By using the modified single-degree-of-freedom (MSDOF) method and validating it against experimental results and finite element method-based analyses, the research shows that a more accurate assessment of damage probability can be achieved compared to the conventional SDOF method. The incorporation of Monte Carlo simulations and Latin Hypercube Sampling underscores the importance of accounting for variability in material properties, geometric features, and load conditions to predict the column's response. Ultimately, this approach contributes to structural engineering practices aimed at enhancing the robustness and reliability of buildings under extreme events like blast, ensuring they can better withstand and recover from such impacts.

Funding statement

This research received no specific grant from any funding agency in the public, commercial, or not-for-profit sectors.

Declaration of competing interest

The authors declare that they have no known competing financial interests or personal relationships that could have appeared to influence the work reported in this paper.

CRediT authorship contribution statement

Mohammad Momeni: Writing – original draft, Validation, Software, Methodology, Investigation, Conceptualization. **Chiara Bedon:** Writing – original draft, Supervision, Software, Methodology, Investigation, Conceptualization. **Mohammad Ali Hadianfard:** Writing – original draft, Supervision, Software, Methodology, Investigation, Conceptualization. **Sina Malekpour:** Writing – original draft, Software, Investigation, Conceptualization.

References

[1] Aghaei M, et al. A study on different failure criteria to predict damage in glass/polyester composite beams under low velocity impact. Steel Compos Struct 2015;18(5):1291–303.
[2] Liu Q, et al. Mechanical behavior of FRP confined steel tubular columns under impact. Steel Compos Struct 2018;27(6):691–702.
[3] Zhao W, et al. Impact response of steel-concrete composite panels: experiments and FE analyses. Steel Compos. Struct. 2018;26(3):255–63.
[4] Figuli L, et al. Experimental mechanical analysis of traditional in-service glass windows subjected to dynamic tests and hard body impact. Smart Struct Syst, Int J 2021;27(2):365–78.
[5] Venkatachari S, Kodur V. Modeling parameters for predicting the fire-induced progressive collapse in steel framed buildings. Resilient Cities Struct 2023;2(3):129–44.
[6] Guerrero JAR, Yang T, Swei O. Earthquake and deterioration inclusive probabilistic life cycle assessment (EDP-LCA) framework for buildings. Resilient Cities Struct 2023;2(3):30–40.
[7] Zhu Z, et al. Objective-level resilience assessment of circular roadway tunnels with reinforced concrete liners for vehicle fire hazards. Resilient Cities Struct 2023;2(3):1–18.
[8] Samadian D, et al. Meta databases of steel frame buildings for surrogate modelling and machine learning-based feature importance analysis. Resilient Cities Struct 2024;3(1):20–43.
[9] Momeni M, et al. Damage investigation of blast loaded UHPFRC panels with optimized mixture design using advanced material models. Results Eng 2024;23:102518.
[10] Mirassi S, Momeni M, Hosseini Moorderaz A. Damage evaluation of concrete bridge with steel piers subjected to explosive loads. J Model Eng 2024;22:297–316.
[11] Rezaei MJ, Gerdooei M, Nosrati HG. Blast resistance of a ceramic-metal armour subjected to air explosion: a parametric study. Struct Eng Mech 2020;74(6):737–45.
[12] Kim DK, Ng WCK, Hwang O. An empirical formulation to predict maximum deformation of blast wall under explosion. Struct Eng Mech 2018;68(2):237–45.
[13] Lotfi1a S, Zahrai SM. Blast behavior of steel infill panels with various thickness and stiffener arrangement. Struct. Eng. Mech 2018;65:587–600.
[14] Husek M, Kala J. Uncertainties in blast simulations evaluated with smoothed particle hydrodynamics method. Struct Eng Mech 2020;74(6):771–87.
[15] Hacıefendioğlu K, et al. Multi-point response spectrum analysis of a historical bridge to blast ground motion. Struct Eng Mech 2015;53(5):897–919.
[16] Mazek SA. Performance of sandwich structure strengthened by pyramid cover under blast effect. Struct Eng Mech 2014;50(4):471–86.
[17] Mussa MH, Mutalib AA, Hao H. Numerical formulation of PI diagrams for blast damage prediction and safety assessment of RC panels. Struct Eng Mech 2020;75(5):607–20.
[18] Amadioa C, Bedon C. FE assessment of dissipative devices for the blast mitigation of glazing façades supported by prestressed cables. Struct Eng Mech 2014;51(1):141–62.
[19] Momeni M, Bedon C, Hadianfard MA. Probabilistic evaluation of steel column damage under blast loading via simulation reliability methods and gene expression programming. Eng Proc 2023;53(1):20.
[20] Nassr AA, et al. Dynamic response of steel columns subjected to blast loading. J Struct Eng 2013;140(7):04014036.
[21] Nassr AA, et al. Single and multi degree of freedom analysis of steel beams under blast loading. Nucl Eng Des 2012;242:63–77.
[22] Nassr AA, et al. Strength and stability of steel beam columns under blast load. Int J Impact Eng 2013;55:34–48.
[23] Magallanes JM, Martinez R, and Koenig JW. Experimental results of the AISC full-scale column blast test. Rep. TR-06, 2006. 20.
[24] Rong H-C, Li B. Probabilistic response evaluation for RC flexural members subjected to blast loadings. Struct Saf 2007;29(2):146–63.
[25] Yokoyama T. Limits to deflected shape assumptions of the SDOF methodology for analyzing structural components subject to blast loading. J Perform Constr Facil 2014;29(5):B4014008.
[26] Crawford JE, Magallanes JM. The effects of modeling choices on the response of structural components to blast effects. Int J Prot Struct 2011;2(2):231–66.
[27] Al-Thairy H. A modified single degree of freedom method for the analysis of building steel columns subjected to explosion induced blast load. Int J Impact Eng 2016;94:120–33.
[28] Lee K, Kim T, Kim J. Local response of W-shaped steel columns under blast loading. Struct Eng Mech 2009;31(1):25–38.
[29] Shi Y, Hao H, Li Z-X. Numerical derivation of pressure–impulse diagrams for prediction of RC column damage to blast loads. Int J Impact Eng 2008;35(11):1213–27.
[30] Hadianfard MA, Farahani A. On the effect of steel columns cross sectional properties on the behaviours when subjected to blast loading. Struct Eng Mech 2012;44(4):449–63.
[31] Hadianfard MA, Nemati A, Johari A. Investigation of steel column behavior with different cross section under blast loading. Modares Civ Eng J 2016;16(4):265–78.
[32] Hadianfard MA, Shekari M. An equivalent single-degree-of-freedom system to estimate nonlinear response of semi-fixed flexural members under impact load. Iran J Sci Technol, Trans Civ Eng, 2018:1–13.
[33] Al-Thairy H. Behaviour and failure of steel columns subjected to blast loads: numerical study and analytical approach. Adv Mater Sci Eng 2018.
[34] Shope RL. Response of wide flange steel columns subjected to constant axial load and lateral blast load. Virginia Tech; 2006.
[35] Ding Y, Song X, Zhu H-T. Probabilistic progressive collapse analysis of steel frame structures against blast loads. Eng Struct 2017;147:679–91.
[36] Stochino F, Attoli A, Concu G. Fragility curves for RC structure under blast load considering the influence of seismic demand. Appl Sci 2020;10(2):445.
[37] Kelliher D, Sutton-Swaby K. Stochastic representation of blast load damage in a reinforced concrete building. Struct Saf 2012;34(1):407–17.
[38] Olmati P, et al. Simplified reliability analysis of punching in reinforced concrete flat slab buildings under accidental actions. Eng Struct 2017;130:83–98.
[39] Stochino F. RC beams under blast load: reliability and sensitivity analysis. Eng Fail Anal 2016;66:544–65.
[40] Hao H, et al. RC column failure probabilities to blast loads. Int J Protect Struct 2010;1(4):571–91.
[41] Hao H, Li Z-X, Shi Y. Reliability analysis of RC columns and frame with FRP strengthening subjected to explosive loads. J Perform Constr Facil 2015;30(2):04015017.
[42] Shi Y, Stewart MG. Spatial reliability analysis of explosive blast load damage to reinforced concrete columns. Struct Saf 2015;53:13–25.
[43] Stewart MG. Reliability-based load factors for airblast and structural reliability of reinforced concrete columns for protective structures. Struct Infrastr Eng 2019;15(5):634–46.
[44] Shi Y, Stewart MG. Damage and risk assessment for reinforced concrete wall panels subjected to explosive blast loading. Int J Impact Eng 2015;85:5–19.
[45] Olmati P, Petrini F, Gkoumas K. Fragility analysis for the performance-based design of cladding wall panels subjected to blast load. Eng Struct 2014;78:112–20.
[46] Low HY, Hao H. Reliability analysis of reinforced concrete slabs under explosive loading. Struct Saf 2001;23(2):157–78.
[47] Low HY, Hao H. Reliability analysis of direct shear and flexural failure modes of RC slabs under explosive loading. Eng Struct 2002;24(2):189–98.
[48] Hussein A, Mahmoud H, Heyliger P. Probabilistic analysis of a simple composite blast protection wall system. Eng Struct 2020;203:109836.

[49] Campidelli M, et al. Blast design-basis threat uncertainty and its effects on probabilistic risk assessment. ASCE-ASME J Risk Uncertain Eng Syst, Part A 2015;1(4):04015012.
[50] Shamim S, Khan RA, Ahmad S. Fragility analysis of masonry wall subjected to blast loading. Structures. Elsevier; 2022.
[51] Borenstein E, Benaroya H. Sensitivity analysis of blast loading parameters and their trends as uncertainty increases. J Sound Vib 2009;321(3):762–85.
[52] Hedayati MH, Sriramula S, Neilson RD. Reliability of profiled blast wall structures. In: Numerical methods for reliability and safety assessment. Springer; 2015. p. 387–405.
[53] Momeni M, Hadianfard MA, Baghlani A. Implementation of weighted uniform simulation method in failure probability analysisof steel columns under blast load. 11th international congress on civil engineering. Iran: University of Tehran; 2018.
[54] Hadianfard MA, Malekpour S, Momeni M. Reliability analysis of H-section steel columns under blast loading. Struct Saf 2018;75:45–56.
[55] Singh K, Gardoni P, Stochino F. Probabilistic models for blast parameters and fragility estimates of steel columns subject to blast loads. Eng Struct 2020;222:110944.
[56] Bogosian D, Ferritto J, Shi Y. Measuring uncertainty and conservatism in simplified blast models. KARAGOZIAN AND CASE GLENDALE CA; 2002.
[57] Netherton MD, Stewart MG. Blast load variability and accuracy of blast load prediction models. Int J Protect Struct 2010;1(4):543–70.
[58] Qi S, et al. Probabilistic blast load model for domes under external surface burst explosions. Struct Saf 2020;87:102004.
[59] Qi S-b, et al. External blast load factors for dome structures based on reliability. Defence Technol 2022;18(2):170–82.
[60] Qi S-b, et al. Sensitivity analysis and probability modelling of the structural response of a single-layer reticulated dome subjected to an external blast loading. Defence Technol 2022;23:152–63.
[61] Mays G, Smith P. Blast effect on building: design of buildings to optimize resistance to blast loading. London, UK: Thos Telford; 1995.
[62] Kinney GF, Graham KJ. Explosive shocks in air. Springer Science & Business Media; 2013.
[63] Borgers J, Vantomme J. Improving the accuracy of blast parameters using a new Friedlander curvature α. DoD explosives safety seminar; 2008.
[64] DoD U. Structures to resist the effects of accidental explosions, Washington, DC, USA: US DoD; 2008. UFC 3-340-02.
[65] Chopra AK. Dynamics of structures: theory and applications to earthquake engineering. Upper Saddle River, NJ: Prentice Hall Inc; 1995.
[66] Humar J. Dynamics of structures. CRC Press; 2012.
[67] Clough Ray W, Penzien J. Dynamics of structures. Computers & structures, Inc; 1995.
[68] Biggs JM, Biggs JM. Introduction to structural dynamics. McGraw-Hill College; 1964.
[69] Bounds WL. Design of blast-resistant buildings in petrochemical facilities. ASCE Publications; 2010.
[70] Cowper GR, Symonds PS. Strain-hardening and strain-rate effects in the impact loading of cantilever beams. Brown Univ Providence RI; 1957.
[71] Regulations B.o.N.B. Iran's national construction regulations, topic twenty-one: passive defense, 2nd ed.. 2016.
[72] Nassr AA. Experimental and analytical study of the dynamic response of steel beams and columns to blast loading. 2012.
[73] Nassr AA, et al. Experimental performance of steel beams under blast loading. J Perform Constr Facil 2011;26(5):600–19.
[74] Momeni M, et al. Damage evaluation of H-section steel columns under impulsive blast loads via gene expression programming. Eng Struct 2020;219:110909.
[75] Momeni M, et al. Numerical damage evaluation assessment of blast loaded steel columns with similar section properties. Structures 2019;20:189–203.
[76] Rubinstein R. Simulation and the Monte Carlo method. New York, NY, USA: John Wiley & Sons, Inc; 1981.
[77] Melchers RE. Structural reliability: analysis and prediction. Horwood; 1987.
[78] Bartlett F, et al. Updating standard shape material properties database for design and reliability (k-Area 4). Technical Report for American Institute of Steel Construction; 2001.
[79] Hadianfard M, Razani R. Effects of semi-rigid behavior of connections in the reliability of steel frames. Struct Saf 2003;25(2):123–38.
[80] Thai H-T, et al. System reliability evaluation of steel frames with semi-rigid connections. J Constr Steel Res 2016;121:29–39.
[81] Ellingwood B. Development of a probability based load criterion for American National Standard A58: building code requirements for minimum design loads in buildings and other structures, 13. US Department of Commerce, National Bureau of Standards; 1980.
[82] Momeni M, et al. An efficient reliability-based approach for evaluating safe scaled distance of steel columns under dynamic blast loads. Buildings 2021;11(12):606.
[83] Song X. Parameterized fragility analysis of steel frame structure subjected to blast loads using Bayesian logistic regression method. Struct Saf 2020;87:102000.
[84] Campidelli M, et al. Inference of blast wavefront parameter uncertainty for probabilistic risk assessment. J Struct Eng 2015;141(12):04015062.
[85] Asprone D, et al. Proposal of a probabilistic model for multi-hazard risk assessment of structures in seismic zones subjected to blast for the limit state of collapse. Struct Saf 2010;32(1):25–34.
[86] Netherton MD, Stewart MG. The effects of explosive blast load variability on safety hazard and damage risks for monolithic window glazing. Int J Impact Eng 2009;36(12):1346–54.
[87] Olmati P, Vamvatsikos D, Stewart MG. Safety factor for structural elements subjected to impulsive blast loads. Int J Impact Eng 2017;106:249–58.
[88] Stewart M, et al. Probabilistic terrorism risk assessment and risk acceptability for infrastructure protection. Aust J Struct Eng 2012;13(1):1–17.
[89] Stewart MG. Reliability-based load factor design model for explosive blast loading. Struct Saf 2018;71:13–23.
[90] Stewart MG, Mueller J. Terror, security, and money: balancing the risks, benefits, and costs of critical infrastructure protection. In: Proc. reliability engineering computing REC 2012; 2012.
[91] Stewart MG, Netherton MD. Security risks and probabilistic risk assessment of glazing subject to explosive blast loading. Reliab Eng Syst Saf 2008;93(4):627–38.
[92] No S. 2800 "Iranian code of practice for seismic resistant design of buildings. Tehran: Third Revision, Building and Housing Research Center; 2010.
[93] Saltelli A, et al.. Sensitivity analysis in practice: a guide to assessing scientific models, 1. Wiley Online Library; 2004.
[94] Saltelli A, Chan K, Scott M. Sensitivity analysis. Sensitivity analysis. John Wiley & Sons publishers; 2000.